Molecular dynamic simulation study of molten caesium

SAEID YEGANEGI[1]*, VAHID MOEINI[2] and ZOHREH DOROODI[2]

[1]*Department of Physical Chemistry, University of Mazandaran, Babolsar, Iran and* [2]*Department of Chemistry, Payame Noor University, P. O. Box 19395-3697, Tehran, Iran*

Abstract: Molecular dynamics simulations were performed to study thermo-dynamics and structural properties of expanded caesium fluid. Internal pressure, radial distribution functions (RDFs), coordination numbers and diffusion coefficients have been calculated at temperature range 700–1600 K and pressure range 100–800 bar. We used the internal pressure to predict the metal––non-metal transition occurrence region. RDFs were calculated at wide ranges of temperature and pressure. The coordination numbers decrease and positions of the first peak of RDFs slightly increase as the temperature increases and pressure decreases. The calculated self-diffusion coefficients at various temperatures and pressures show no distinct boundary between Cs metallic fluid and its expanded fluid where it continuously increases with temperature.

Keywords: metal–non-metal transition; MD simulation; internal pressure; RDF.

INTRODUCTION

Molten Cs has been attracted considerable attention for its novel properties which makes it potentially useful in the systems which need heat pipe, lubricants and coolants at high temperature. Also, it is used in space and nuclear power technology.[1–4] Experimental and theoretical investigations show that a momentous amount of clustering takes place in the region of the metal-nonmetal transition, when the density decreases below 1.3 g cm^{-3}.[5–7] The design and development of technological applications of Cs, as a kind of new engineering material, needs a precise knowledge of the structural and dynamical features of alkali metal fluids. The metal–non-metal transition for alkali metals occurs close to critical point,[8] but does not coincide with it.[9]

Because of the experimental difficulty at high pressure and temperature (the critical point of liquid- vapor transitions for Cs is T_c = 1924 K, p_c = 9.25 MPa and d_c = 0.38 g cm^{-3}),[10] the simulation can be used as a valuable method to study metallic fluids. One of the early efforts to study the structure of liquid metals was

performed in 1952[11] and the first momentous molecular dynamics (MD) simulation for Cs was performed in 2001.[12] The diffusion and shear-viscosity coefficients and velocity auto correlation function have been reported for Na, K, Rb and Cs near the melting point.[13–15] The simple but useful expressions for the relationship between structural and surface properties of liquid metals have been presented by employing the hard-sphere description near the melting point.[16,17] Also, MD simulations have been performed to calculate the structural and transport properties of liquid alkali metals by using reformed Morse potential near the melting point.[18] The embedded atom method potentials have been calculated for the alkali metals along the melting line of the metal and the discrepancy between the simulated energy, and the actual energy of the metal at high temperatures has been discussed.[19] Recently, thermodynamic quantities of the alkali metals[20] and their cluster size distributions[21] have been studied based on the static crystalline properties and using *ab initio* potential respectively.

Gupta proposed a semi-empirical potential to study the metallic fluids by molecular dynamics.[22] The Gupta potential function has been applied successfully by many researchers to describe the structure and energy of Pb[23], Ni, Ag, Au[24] and Cu–Au, Al, Zn and Cd clusters.[25] Also, Gupta potential has been used to study the melting of Na and Cs clusters in order to investigate the effects of the geometric and electronic magic numbers on the melting temperature as a function of cluster size.[26–28]

The electronic structure of alkali metal fluids strongly depends on the thermodynamic state of the system. When Cs fluid expands, two transitions can occur, liquid–vapour and metal–non-metal one.[9] In fact, a high-density liquid metal is a conductor, while it becomes a non-metal insulator when turned into low-density vapour. Near the critical point the transition from a liquid metal to a non-metal takes place.[29] This transition implies that the nature of the particle interactions must change dramatically, from metallic to a van der Waals-type interaction.[30]

The particle interactions in dense alkali metals are dominated by the Coulomb potential, whereas the interactions in the nonmetallic phase are weak van der Waals forces. It is suggested that there is a relationship between rapid variation in the conductivity and density.[31] The metal–non-metal transition can be investigated by comparing the measured electrical conductivity with the value calculated from the nearly-free-electron theory (NFE). This theory is often used to describe metallic behaviour and is valid when the mean free path of the conduction electron is much larger than the average distance between neighbouring atoms in the liquid. It has been shown that the nearly-free electron theory provides a good account of the conductivity for Cs for densities higher than 1.3 g cm^{-3}.[29–31] According to this theory, the transition begins at 1.3 g cm^{-3} for Cs, which is exactly the density around which the deviation from the linear isotherm

regularity (LIR) is observed.[5,32] Keshavarzi *et al.*[32] demonstrated that the metal––non-metal transition is surely neither first nor second order, and it can occur separately or simultaneously with the liquid–vapour transition (LVT). In other words, the metal–non-metal transition proceeds gradually, which is indicated by some changes in liquid properties such as lower conductivity than that predicted by NFE theory,[29,30] deviation of density from the LIR predictions for a single phase.[5,32]

There has been an increasing interest in the study of internal pressure in the elucidation of thermodynamic properties of metallic fluids.[5] A general method of calculating the internal pressure is based on the thermodynamic equation of state:

$$p_i = \left[\frac{\partial E}{\partial V}\right]_T = T\left[\frac{\partial p}{\partial T}\right]_V - p \tag{1}$$

E is the internal energy, $\left[\partial E / \partial V\right]_T$ is the internal pressure and $T\left[\partial p / \partial T\right]_V$ is usually called the thermal pressure.[33–35] According to the statistical mechanics, the total internal energy E of a fluid is the sum of potential energy, U, and the kinetic energy, K. It is assumed that any kinetic energy contribution to the internal energy will vanish on taking the derivative, since the temperature is held constant.[36] The potential energy can be divided into two parts, attractive U_A and repulsive U_R parts[37] and inserting into Eq. (1) gives:

$$p_i = \left(\frac{\partial (U+K)}{\partial V}\right)_{N,T} = \left(\frac{\partial (U_A + U_R)}{\partial V}\right)_{N,T} = p_{i,A} + p_{i,R} \tag{2}$$

Where $p_{i,A}$ is the attractive internal pressure (positive) and $p_{i,R}$ is the repulsive internal pressure (negative). As the density is raised at constant temperature, the repulsive pressure becomes predominant, and therefore, internal pressure decreases. On the other hand, the reason is that the resultant forces under low pressure conditions are attractive, and as the pressure increases, the repulsive forces become predominant.

Although some approximate approaches exist, there is no definite way to distinguish the metallic and non-metallic states. Moeini[5] has shown that linear regularity of simple fluid can be applied successfully for predicting the metal––non-metal transition in alkali metals. Based on this assumption they showed that internal pressure of expanded Cs versus density has a maximum around 1.3 g cm^{-3} or 0.097 L mol^{-1}, when before reaching this density some properties such as local contraction, electrical conductivity and magnetic susceptibility show significant changes.[5,9,29,30,31]

Internal pressure, as well as density, of molten metal can be used to recognize the metal–non-metal transition of an expanded metallic fluid.[32,33] The goal of this paper is the study of the pressure dependence of internal pressure of Cs fluid

by the molecular dynamics (MD) simulations to recognize the initiation of metal–non-metal transition from the bulk fluid up to the expanded fluid. MD simulations were performed near metal-nonmetal transition by using Gupta potential. In the present work, up to our knowledge, we demonstrate the first study to calculate internal pressure by performing classical molecular dynamics. We used the internal pressure in order to predict metal–non-metal transition and also we study the structural and dynamical properties from bulk up to creating expanded fluid of Cs by calculation of radial distribution function, coordination number and diffusion coefficient.

SIMULATION DETAILS

We have used Gupta potential to describe the interactions in Cs fluid. Based on this potential, the energy between particles can be written as a sum of Born-Mayer-type repulsive and many-body attractive energies as:[38]

$$E = \sum_{j \neq i} A \exp(-p\frac{r_{ij}}{r_0} - 1) - \left(\sum_{j \neq i} B^2 \exp[-2q(\frac{r_{ij}}{r_0} - 1)] \right)^{0.5} \quad (3)$$

where r_{ij} is distance between i and j atoms and r_0 is the equilibrium nearest-neighbour distance in the bulk fluid. The parameters p and q represent the repulsive interaction and the attractive interaction ranges, respectively. The Gupta potential parameters for Cs used in this work are: $A = 0.02054$ eV, $B = 0.24218$ eV, $p = 9.62$, $q = 1.45$ and $r_0 = 9.44$ a.u.[24]

Cs and other alkali metals are simple metals, meaning that the Fermi surface of these metals is spherical. They are generally considered to be monatomic simple liquids.[39,40] In all our molecular dynamic simulations, we have used 428 Cs atoms initially placed in a bcc array replicated in *xyz* directions. All MD simulations were performed using DL-POLY-2.18 program.[41]

Internal pressure and radial distribution function (RDF) were calculated at wide ranges of temperature (700, 800, 900, 1000, 1100, 1200, 1300, 1400, 1500 and 1600 K) and pressure (100, 200, 300, 400, 500, 600, 700 and 800 bar). At each temperature for the lowest pressure, 428 atoms were placed in the simulation cell then NPT (constant particle number, pressure and temperature) simulation was conducted for 5ns with the Berendsen method using 1 and 3 ps as the thermostat and barostat relaxation times to reproduce the experimental density.[42] The equations of atomic motion was integrated using the Verlet velocity algorithm[43] with a time step of 0.005 ps and cut off distance of 12.0 Å. The diffusion coefficients were calculated by NVT MD simulations and Berendsen thermostat for 10 ns time steps where 2 ns steps were discarded as equilibration.

RESULTS AND DISCUSSION

Internal pressure

The calculated total energy and density are presented and compared with experimental densities[42] in Table I. The deviations expressed in percent from experimental values are shown in Fig. 1. Our simulations underestimate Cs density for temperatures higher than 900 K while overestimating it for lower temperatures. Large deviation at high temperatures and low pressures can be attributed

to the lack of sufficient accuracy of the proposed potential energy function to describe the atomic interactions. Also, the large fluctuation in density due to the formation and destruction of varying size Cs clusters at low pressure and high temperatures can be the cause for the observed large deviations.

TABLE I. Calculated total energy, E, calculated density, d_{cal}, and experimental density, d_{exp}, of Vargaftik et al.[42] for Cs fluid at different pressures, p, and temperatures, T

p / bar	E / J mol^{-1}	d_{cal} / g cm^{-3}	d_{exp} / g cm^{-3}	p / bar	E / J mol^{-1}	d_{cal} / g cm^{-3}	d_{exp} / g cm^{-3}
	T = 700 K				T = 800 K		
100	−559.263	1.662	1.626	100	−530.899	1.579	1.57
200	−561.786	1.685	1.643	200	−534.217	1.606	1.588
300	−564.169	1.706	1.659	300	−537.114	1.630	1.605
400	−566.366	1.727	1.675	400	−539.684	1.653	1.622
500	−568.235	1.747		500	−542.02	1.675	
600	−569.917	1.765	1.704	600	−544.053	1.695	1.654
700	−571.529	1.783		700	−546.062	1.715	
800	−572.931	1.800		800	−547.838	1.733	
	T = 900 K				T = 1000 K		
100	−502.372	1.496	1.515	100	−473.167	1.410	1.457
200	−506.437	1.526	1.533	200	−478.377	1.446	1.477
300	−509.965	1.554	1.552	300	−482.886	1.479	1.497
400	−513.026	1.579	1.570	400	−486.624	1.508	1.516
500	−516.04	1.604		500	−490.082	1.534	
600	−518.563	1.627	1.604	600	−493.05	1.559	1.554
700	−520.759	1.648		700	−495.993	1.584	
800	−522.955	1.669		800	−498.4	1.606	
	T = 1100 K				T = 1200 K		
100	−443.097	1.321	1.397	100	−412.117	1.229	1.335
200	−449.943	1.365	1.419	200	−420.458	1.280	1.361
300	−455.387	1.402	1.441	300	−427.654	1.325	1.385
400	−460.106	1.435	1.463	400	−433.355	1.363	1.409
500	−464.195	1.466		500	−438.284	1.397	
600	−467.863	1.494	1.504	600	−442.49	1.428	1.454
700	−471.017	1.519		700	−446.228	1.456	
800	−473.914	1.544		800	−449.639	1.483	
	T = 1300 K				T = 1400 K		
100	−378.87	1.127	1.272	100	−343.006	1.017	1.204
200	−390.388	1.193	1.301	200	−359.057	1.102	1.240
300	−399.103	1.245	1.328	300	−370.038	1.164	1.271
400	−406.182	1.289	1.354	400	−378.706	1.216	1.299
500	−412.093	1.328		500	−385.809	1.260	
600	−417.163	1.363	1.404	600	−391.673	1.298	1.354
700	−421.509	1.394		700	−396.79	1.332	
800	−425.364	1.423		800	−401.323	1.364	
	T = 1500 K				T = 1600 K		
100	−302.376	0.888	1.131	100	−251.747	0.724	1.052
200	−325.694	1.005	1.175	200	−290.344	0.902	1.108

TABLE I. Continued

p / bar	E / J mol^{-1}	d_{cal} / g cm^{-3}	d_{exp} / g cm^{-3}	p / bar	E / J mol^{-1}	d_{cal} / g cm^{-3}	d_{exp} / g cm^{-3}
	$T = 1500$ K				$T = 1600$ K		
300	−340.413	1.083	1.211	300	−309.362	0.997	1.149
400	−351.02	1.142	1.244	400	−322.469	1.067	1.187
500	−359.314	1.191		500	−332.609	1.123	
600	−366.02	1.233	1.305	600	−340.553	1.170	1.256
700	−372.188	1.272		700	−347.352	1.212	
800	−377.188	1.306		800	−353.193	1.249	
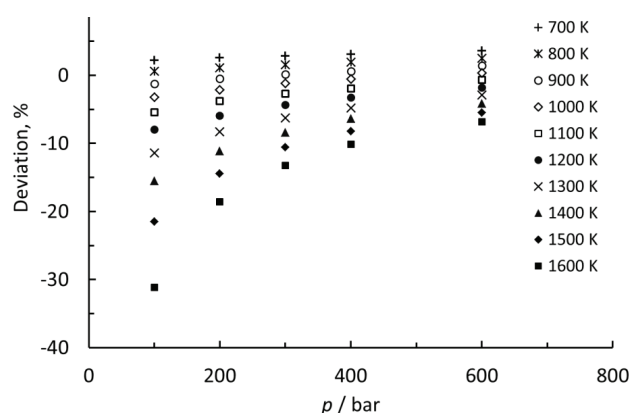
Fig. 1. Relative deviations of calculated densities from the experimental values[42] from Table I for Cs at temperature range 700–1600 K.

Internal energy is generally represented by a cubic expression in the density by allowing the coefficients to depend on temperature.[34] We have used a similar expression in terms of volume rather than density:

$$E = E_0 + aV + bV^2 + cV^3 \tag{4}$$

where $V = V(p,T)$ and a, b and c are constants characteristic of a particular substance. The fitting parameters a, b and c can be determined by fitting E *versus* V at constant temperature over the whole pressure range. Fitted parameters are shown in Table II, while coefficients of determination (R^2) for all of fittings were nearly 1. After the seminal work of Parsafar[34] many researcher used the equation $U = U(V)$ for obtaining the equation of state and some linear regularities (LIR).[36] Up to our knowledge, we obtained for the first time the coefficients of $U = U(V)$ by fitting the calculated internal energies to volume. The obtained coefficients are strongly depended on temperature, which shows the dependence of the interparticle interaction to the thermodynamic sate of the Cs. The calculated internal energy from Eq. (4) and the simulated one depicted good agreement in Fig. 2. The internal pressure can be obtained by the straightforward differentiation of internal energy with respect to volume at constant temperature.

TABLE II. Fitted parameters of equation 4, *a, b, c* at different temperatures *T*

T / K	a / kJ mol^{-1} m^{-3}	b / 10^7 kJ mol^{-1} m^{-6}	c / 10^{12} kJ mol^{-1} m^{-9}
700	−3.71	675.07	394.49
800	0.19	−24.95	23.36
900	−0.96	175.57	−93.48
1000	−0.21	52.18	−26.18
1100	−0.34	71.57	−36.16
1200	−0.34	69.14	−34.43
1300	−0.09	32.16	−16.59
1400	0.07	10.44	−6.78
1500	0.15	−0.52	−2.08
1600	0.23	−9.53	1.40
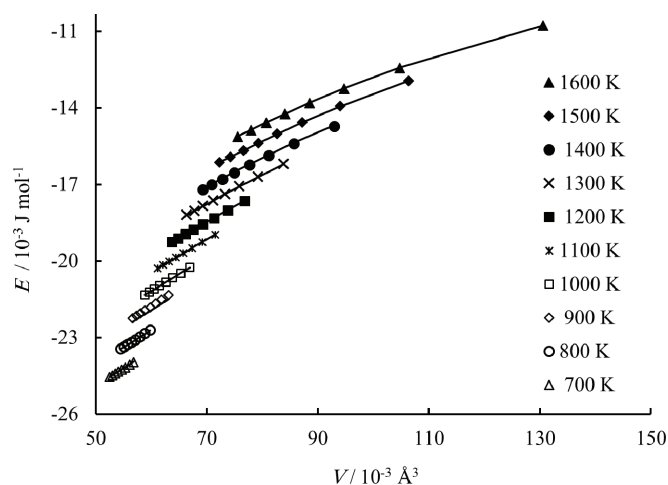
Fig. 2. Calculated (symbols) and simulated (lines) internal energies *vs.* volume for Cs.

The resulting internal pressures, p_i, versus molar volume are shown in Fig. 3. It shows that at 700–1000 K, internal pressure, p_i, increases with molar volume, V_m, but for 1300–1600 K, it decreases with molar volume. The isotherms of 1100 and 1200 K in Fig. 3 show maxima at about 0.093 and 0.094 L mol^{-1} (1.43 and 1.41 g cm^{-3}), respectively. Our results are in agreement with previous experimental and theoretical results[5,6,44,45] which showed that the internal pressure had a maximum at 1.3 g cm^{-3} (0.097 L mol^{-1}) at 1350 K. It is well known that liquid Cs at high densities shows characteristics typical of a nearly free electron (NFE) metal.[6,31,44,46] However, when the density is reduced below about 1.3 g cm^{-3} or the temperature is increased up to 1350 K, the quantitative changes begins to develop. Under this condition, the measured electrical conductivity is lower than the NFE value[31] and the magnetic susceptibility[47] and density fluctuation[48] increase. These changes indicate that the metal–non-metal transition is developing and that it is strongly dependent on the thermodynamic state.[29–31] The failure of the
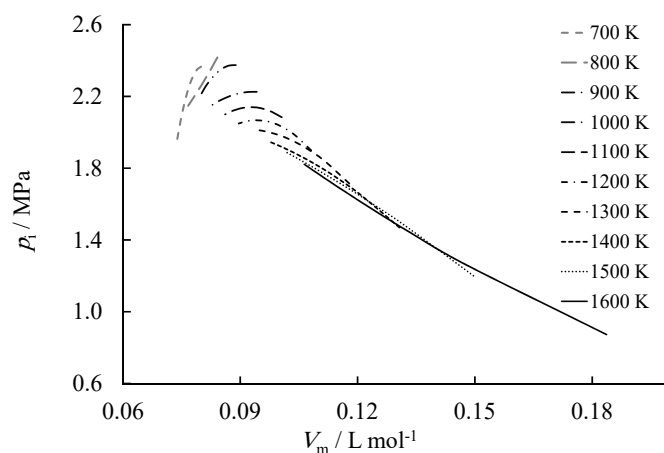
Fig. 3. Calculated internal pressure p_i isotherms for Cs at temperature range 700–1600 K.

NFE theory reflects, most probably, cluster formation and the increased importance of soft potential.[5,6,31,45] It is revealed that for molar volumes higher than V_{max} the attractive force becomes predominant and it has strong influence on the determination of internal energy and internal pressure.[6,32,48,49] Marcus[50,51] has shown that the internal pressure of water (contrary to most liquids, except liquid metals) increases with the temperature and exhibit a maximum at 446.15 K. He has explained this behaviour in terms of gradual change in the nature of binding between water molecules. Likewise, the maximum in internal pressure *vs*. molar volume in Fig. 2 can be understood in terms of two different bindings in the molten alkali metals.[32] At the low molar volumes (high pressures and low temperatures), where the measured conductivity and thermodynamic state of the system agrees well with predictions from the NFE theory and the LIR, respectively,[5,6,27,32] the system is in a monoatomic state with a delocalized electron cloud over the entire system. In this state, increasing the molar volume further (decreasing pressure) leads to a smaller repulsion between ions and negative repulsive internal pressure, $p_{i,R}$, which tend to increases the internal pressure. As can be seen from Fig. 2 at 700 K, the internal pressure increases steadily with the increasing the molar volume. Further increasing of the molar volume leads to clustering, where the electrons tend to be shared between atoms within a cluster, resulting in a molecular or polyatomic structure with an insignificant conductivity. Therefore, there are two different types of bindings in the system, the metallic bonding between atoms within clusters and van der Waals attractions between clusters. Formation of clusters diminish the metallic bonding then decreases the attraction energy over the system where this decreases the attractive internal pressure, $p_{i,A}$. Keshavarzi *et al*.[32] have shown that this transition is neither first nor second order but occurs gradually in the expanded molten Cs. The max-

imum of internal pressure in Fig. 3 is the point where the electron delocalization over the entire system breaks down by clustering and the system composed of the metallic and non-metallic parts.

The extrapolation of results of a rather small system to bulk fluid must be done carefully. In order to check the size dependency of our results, especially the location of V_{max}, the internal pressures versus molar volume at 1100 K were reproduced for a larger system with 856 Cs atoms in Fig. 4 and compared with that of a smaller system. Figure 4 revealed that the density for a larger system is shifted slightly toward smaller molar volume but the location of the maximum remains nearly unchanged. So, one can conclude that the value of V_{max} is independent of the system size.
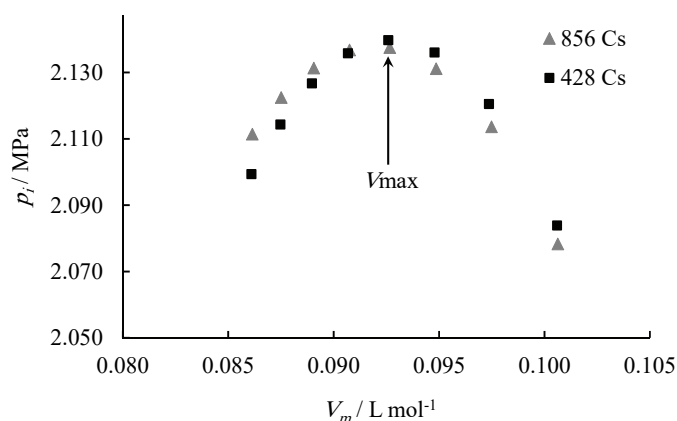

Fig. 4. Calculated internal pressure, p_i, for 428 (black square) and 856 Cs atoms (grey triangle) at 1100 K.

Fluid structure

We calculated radial distribution functions (RDFs) of the expanded Cs in whole studied temperature and pressure ranges using Gupta potential. The positions of the first peak of RDFs, namely r_{max}, have been analysed. It slowly rises from 4.98 Å at low temperature and high pressure, to 5.03 Å at high temperature and low pressure. The RDFs at temperature range 700–1600 K and 500 bar pressure are plotted as an example in Fig. 5. It shows that the intensity of the first and second peak of RDFs reduced and overspread as temperature increases.

The coordination number, N, up to the first minimum of RDFs for Cs fluid is plotted in Fig. 6 at the studied temperature and pressure ranges. The calculated coordination number generally decreases with temperature, from 12 to 7, but its variations are strongly depends on the thermodynamic state of the system. The variations of the coordination number at high temperature and low pressure are more pronounced than in the low temperature and high pressure.
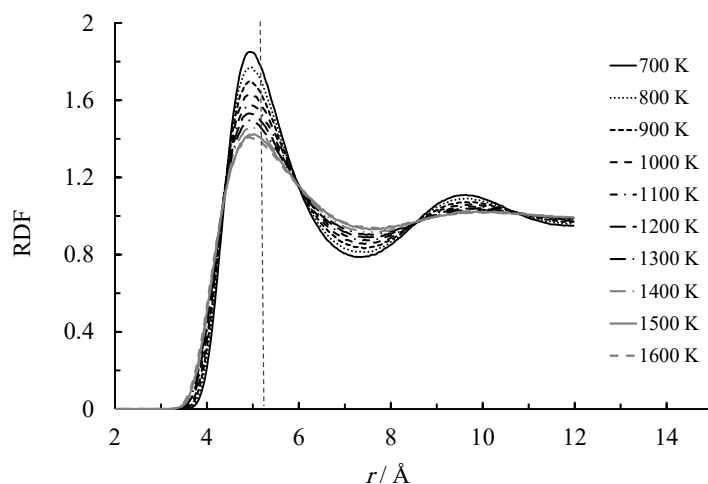
Fig. 5. Radial distribution functions (RDFs) for Cs at p = 500 bar at temperatures from
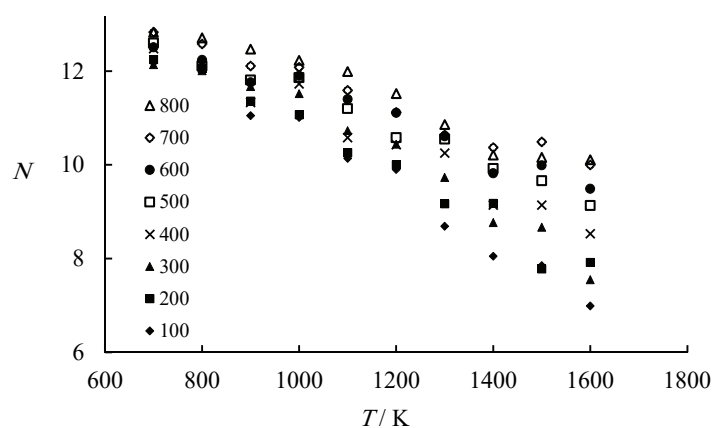700 to 1600 K.

Fig. 6. The calculated coordination number (N) of Cs at temperatures from 700 to 1600 K and
pressures from 100 to 800 bar.

The comparison of snapshots of the system at low and high temperatures in
Fig. 7 shows that, as the system expands, the average nearest neighbour-distance
(r_{max}) remains nearly constant while the average coordination number decreases.
This observation agrees well with the findings of Hensel[30] explained based on the
formation of Cs clusters. The average coordination number decreases because of
an increase in the number of atoms on the surface of clusters.[30] This calculations
are in good agreement with the results of previous studies.[7,29,47] Our study shows
that in high temperature, when non-metallic properties are prevailing, the coor-
dination number of Cs fluid is less than 11, while it is larger than 11 for Cs fluid
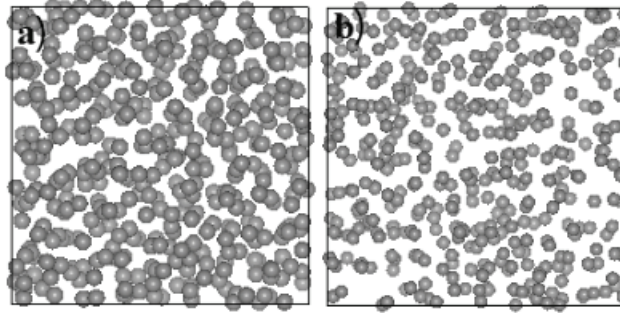with metallic properties at lower temperature.

Fig. 7. Snapshots of the simulation ensemble at: a) $T = 700$ K and $p = 800$ bar and b) $T = 1500$ K and $p = 100$ bar.

Self-diffusion coefficient

The knowledge of diffusivities plays an important role in the investigation of liquid metals and fluids. Numerous experimental and theoretical diffusion coefficient data exist near melting point of Cs [13,14,16,18] and a few studies of liquid metals have been carried out at high temperature.[29,52,53] However, for temperature and pressure ranges considered here, there is no reported diffusion coefficient for Cs fluid. The diffusion coefficients were calculated for some selected points around the maximum of the p_i–V_m curve in Fig. 3 and reported in Table III. The state of Cs fluid for molar volumes lower and higher than V_{max} were labelled M and EM, respectively. The state of the maximum points of p_i–V_m isotherm curves at 1100 K and 400 bar are shown also in Table III. The entries in Table III were sorted based on the diffusion coefficient increment. The inspection of Table III shows that although there is not a definite boundary between metal and non--metal regions, one can certainly predict that the compressed Cs fluid with diffusion coefficient less than 9.12×10^{-6} cm^2 s^{-1} possess metallic characteristic and the expanded Cs with diffusion coefficient greater than 1.07×10^{-5} cm^2 s^{-1} starts to show non-metallic characteristic. So one can suggest the diffusion coefficient as a simple factor to characterize the metallic state of Cs fluid. Calculated diffusion coefficients of metallic and non-metal Cs are different by one order of magnitude, but the metal to non-metal transition takes place gradually in terms of diffusion coefficient.

TABLE III. Calculated molar volume, V_m, coordination number, N, diffusion coefficient, D, and state of the Cs fluid designated as metal (M) or expanded metal (EM) around maximum point (MAX) of p_i–V_m in Fig. 3

T / K	p / bar	V_m / L mol^{-1}	N	D / 10^6 cm^2 s^{-1}	State
700	800	0.074	12.83	3.96	M
700	600	0.075	12.51	4.14	M
800	100	0.084	12.08	6.07	M

TABLE III. Continued

T / K	p / bar	V_m / L mol^{-1}	N	D / 10^6 cm^2 s^{-1}	State
900	100	0.089	11.05	7.45	M
1100	800	0.086	11.99	8.55	M
1100	600	0.089	11.41	8.92	M
1000	200	0.092	11.07	9.07	M
1100	500	0.091	11.20	9.12	M
1100	400	0.093	10.58	9.45	MAX
1000	100	0.094	11.01	9.60	M
1100	300	0.095	10.73	10.19	EM
1200	800	0.090	11.52	10.45	M
1200	700	0.091	11.12	10.46	M
1200	600	0.093	11.11	10.65	M
1100	100	0.100	10.14	10.73	EM
1200	500	0.095	10.58	11.36	EM
1200	400	0.097	10.44	11.42	EM
1300	800	0.093	10.86	11.43	EM
1400	800	0.097	10.21	13.40	EM
1500	800	0.102	10.16	14.94	EM
1600	700	0.110	10.00	18.09	EM
1600	100	0.184	6.99	21.37	EM

CONCLUSIONS

We calculated density, internal pressure, RDFs and diffusion coefficients of Cs fluid using molecular dynamics and Gupta potential for wide ranges of pressure and temperature to investigate the metal–non-metal transition. The internal pressure of Cs fluid exhibits a pronounced maximum when the transition from metal to non-metal begins to develop. Our results showed that molten Cs with coordination number more than 11 exhibits metallic behaviour, while for the expanded fluid of Cs, with lower electrical conductivity than predicted by NFE theory, the coordination number is less than 11. The dynamical behaviour of Cs fluid was studied by the calculation of self-diffusion coefficients. Our results show that the diffusion coefficients of metallic Cs are smaller than those of the expanded fluid. It is shown that the diffusion coefficient can be used to characterize the metallic and non-metallic state of Cs fluid accurately, although it is not as accurate as internal pressure.

И З В О Д

СТУДИЈА СТОПЉЕНОГ ЦЕЗИЈУМА МОЛЕКУЛСКО-ДИНАМИЧКОМ СИМУЛАЦИЈОМ

SAEID YEGANEGI[1], VAHID MOEINI[2] и ZOHREH DOROODI[2]

[1]Department of Physical Chemistry, University of Mazandaran, Babolsar, Iran и [2]Department of Chemistry, Payame Noor University, P. O. Box 19395-3697, Tehran, Iran

Урађене су симулације молекулском динамиком са циљем да се проуче термодинамичка и структурна својства експандованог течног Cs. Унутрашњи притисак, функције радијалне расподеле (RDFs), координациони бројеви и коефицијенти дифузије израчу-

нати су у температурном опсегу 700−1600 K и опсегу притиска 100−800 bar. Користили смо унутрашњи притисак за предвиђање области појављивања прелаза метал–неметал. RDF су израчунате за широке области температуре и притиска. Координациони бројеви опадају, а положаји првог пика у RDF лагано расту са порастом температуре и са смањењем притиска. Израчунати коефицијенти самодифузије на различитим температурама и притисцима не показују за Cs јасну границу између металног и експандованог течног стања, а континуално расту са температуром.

REFERENCES

1. C. T. Ewing, J. P. Spann, J. R. Stone, R. R. Miller, *J. Chem. Eng. Data* **16** (1971) 27
2. C. T. Ewing, J. R. Spann, J. P. Stone, E. W. Steinkuller, R. R. Miller, *J. Chem. Eng. Data* **55** (1971) 508
3. W. D. Weatherford, R. K. Johnston, M. L. Valtierra, *J. Chem. Eng. Data* **9** (1964) 520
4. F. Roehlich, F. Tepper, R. L. Rankin, *J. Chem. Eng. Data* **13** (1968) 518
5. V. Moeini, *J. Chem. Eng. Data* **55** (2010) 1093
6. K. Matsuda, S. Naruse, K. Hayashi, K. Tamura, M. Inui, Y. Kajihara, *J. Phys.: Conf. Series* **98** (2008) 012003
7. V.M. Nield, M.A. Howe, R. L. McGreevy, *J. Phys.: Condens. Matter* **3** (1991) 7519
8. R. Winter, F. Noll, T. Bodensteiner, W. Glaser, P. Chieux, F. Hensel, *Z. Phys. Chem.* **156** (1988) 145
9. H. Z. Zhuang, X.-W. Zou, Z.-Z. Jin, D.-C. Tian, *Physica, B* **253** (1998) 68
10. S. Jungst, B. Knuth, F. Hensel, *Phys. Rev. Lett.* **55** (1985) 2160
11. F.C. Frank, *Proc. R. Soc. Lond., A* **215** (1952) 43
12. A. Agoado, *Phys. Rev., B* **63** (2001) 115404
13. U. Balucani, A. Torcini, R. Vallauri, *Phys. Rev., B* **47** (1993) 3011
14. J-F. Wax, R. Albaki, J.-L. Bretonnet, *J. Non Cryst. Solids* **312**–**314** (2002) 187
15. J.K. Baria, A. R. Jani, *J. Non Cryst. Solids* **356** (2010) 1696
16. I. Yokoyama, *Physica, B* **291** (2000) 145
17. N. Farzi, R. Safari, F. Kermanpoor, *J. Mol. Liquids* **137** (2008) 159
18. F. Juan-Coloa, D. Osorio-Gonzalez, P. Rozendo-Francisco, J. Lopez-Lemus, *Mol. Simul.* **33** (2007) 1162
19. D. Belashchenko, *Inorg. Mater.* **48** (2011) 79
20. A. Nichol, G. J. Ackland, *Phys. Rev., B* **93** (2016) 184101
21. V. V. Chaban, O. V. Prezhdo, *J. Phys. Chem., A* **120** (2016) 4302
22. R.P. Gupta, *Phys. Rev., B* **23** (1981) 6265
23. J.P.K. Doye, *Comput. Mater. Sci.* **35** (2006) 227
24. K. Michaelian, N. Rendon, I. L. Garzon, *Phys. Rev., B* **60** (1999) 2000
25. K. Michaelian, M. R. Beltran, I. L. Garzon, *Phys. Rev., B* **65** (2002) 041403.
26. M. Manninen, K. Manninen, A. Rytkönen, in: *Latest Advances in Atomic Cluster Collisions,* J. P. Connerade, A. V. Solov'yov, Eds., World Scientific, Imperial College Press, London, 2004, p. 33
27. M. H. Ghatee, K. Shekoohi, *Fluid Phase Equilib.* **327** (2012) 14
28. J. A. Reyes-Nava, I. L. Garzion, M. R. Beltrian, K. Michelian, *Rev. Mex. Fis.* **48** (2002) 450
29. R. Winter, C. Pilgrrim, F. Hensel, *J. Phys. IV* **1** (1991) 45
30. F. Hensel, in: *High Pressure Chemistry, Biochemistry and Materials Science*, R. Winter, J. Jonas, Eds., NATO ASI Series, Springer, Aquafredda di Maratea, 1993, p. 401

31. F. Hensel,W.-C. Pilgrim, *Int. J. Mod. Phys., B* **6** (1992) 3709
32. E. Keshavarzi, G. Parsafar, *J. Phys. Chem., B* **103** (1999) 6584
33. V. Moeini, *J. Chem. Eng. Data* **55** (2010) 5673
34. G. Parsafar, E. A. Mason, *Phys. Rev., B* **49** (1994) 3049
35. J. O. Hirschfelder, C. F. Curtiss, R. B. Bird, *Molecular Theory of Gases and Liquids,* John Willey & Sons, Inc, New York, 1964, p. 647
36. G. Parsafar, E. A. Mason, *J. Phys. Chem.* **97** (1993) 9048
37. I. N. Levine, *Physical Chemistry*, McGraw Hill, New York, 2002, p. 55
38. F. Cleri, V. Rosato, *Phys. Rev., B* **48** (1993) 22
39. N. W. Ashcroft, N. D. Mermin, *Solid state Physics*, Holt, Rinehart and Winston, New York, 1976, p. 284
40. N. H. March, *Liquid Metals: Concepts and Theory*, Cambridge University Press, Cambridge, 1990, p. 155
41. I. T. Todorov, W. Smith, K. Trachenko, M.T. Dove, *J. Mater. Chem.* **16** (2006) 1911
42. N. B. Vargaftik, E. B. Gelman, V. F. Kozhevnikov, S. P. Naursakov, *Int. J. Thermophys.* **11** (1990) 467
43. M. P. Allen, D. J. Tildesley, *Computer Simulation of Liquids*, Clarendon Press, Oxford, 1989, p. 81
44. M. H. Ghatee, M. Bahadori, *J. Phys. Chem., B* **105** (2001) 11256
45. V. F. Kozhevnikov. S. P. Naurzakov, A. P. Senchenkov, *J. Moscow Phys. Soc.* **1** (1991) 171
46. V. Moeini, *J. Phys. Chem., B* **110** (2006) 3271
47. W. Freyland, *Phys. Rev., B* **20** (1979) 5104
48. K. Matsuda, K. Tamura, M. Inui, *Phys. Rev. Lett.* **98** (2007) 096401
49. K. Tamura, K. Matsuda, M. Inui, *J. Phys.: Condens. Matter* **20** (2008) 114102
50. Y. Marcus, *Chem. Rev.* **113** (2013) 6536
51. Y. Marcus, *J. Mol. Liquids* **79** (1999) 151
52. J. Yuan-Yuan, Z. Qing-Ming, G. Zi-Zheng, J. Guang-Fu, *Chin. Phys., B* **22** (2013) 083101
53. A. K. Metya, A. Hens, J. K. Singh, *Fluid Phase Equilib.* **313** (2012) 16.